Original Article
Senomorphic agent pterostilbene ameliorates osteoarthritis through the PI3K/AKT/NF-κB axis: an in vitro and in vivo study

Yu Wang[1,2*], Huai Zhao[3*], Shuangshuo Jia[1], Qian Wang[2], Wuyi Yao[2], Yue Yang[1], Lunhao Bai[1]

[1]Department of Orthopedic Surgery, Shengjing Hospital Affiliated China Medical University, Shenyang 110004, Liaoning, PR China; [2]Department of Orthopedics Surgery, Affiliated Hospital of Chengde Medical College, 36 Nanyingzi Street, Shuangqiao District, Chengde 067000, Hebei, PR China; [3]Department of General Surgery, Shengjing Hospital Affiliated China Medical University, Shenyang 110004, Liaoning PR China. *Equal contributors and co-first authors.

Abstract: Objectives: Osteoarthritis (OA) is the most common joint disease in the world. Among the many risk factors for OA, aging is one of the most critical factors. The treatment with senop-associated secretory phenotype (SASP) is one of the important, promising anti-aging strategies at present. Pterostilbene (PTE) is a trans-stilbene compound with anti-tumor, anti-oxidation, anti-inflammatory, and anti-aging pharmacologic activities. The purpose of this study is to explore the therapeutic effects of PTE on articular chondrocyte senescence and OA and its related mechanisms. Methods: Male Sprague-Dawley rats were operated on with transection of the anterior cruciate ligament (ACLT) and a destabilized medial meniscus (DMM) surgery to establish the OA model and then injected intraperitoneally with PTE (20 mg/kg) for 5 weeks. Finally, rats were sacrificed and knee joints were collected for histologic analysis. Rat chondrocytes were stimulated with interleukin-1β (IL-1β) with or without PTE treatment. The therapeutic effects of PTE and related mechanisms were investigated by examining and analyzing relative markers through senescence-associated β-galactosidase (SA-β-Gal) assay, cell cycle, qRT-PCR, western blot, bioinformatic analysis, immunofluorescence, and molecular modeling. Results: With in vivo experiments, PTE can significantly reduce the Mankin scores and OARSI scores of the knee joint in ACLT+DMM OA model rats and reduce the interleukin-6 (IL-6) level in the knee lavage fluid. Immunohistochemical staining showed that compared to the OA group, the PTE treatment group had significantly increased expression of collagen type II in articular cartilage, and significantly decreased matrix metalloproteinase 13 (MMP-13) and IL-6, the main SASP proteins, and had expression of p16 and p21, markers of aging in chondrocytes. In vitro, PTE reduced the ratio of SA-β-Gal positive chondrocytes and G0-G1 phase chondrocytes in IL-1β-induced rat chondrocytes. PTE significantly inhibited the expression of MMP-13, IL-6, thrombospondin motif 5 (ADAMTS5), p16, and p21, and significantly increased the expression of collagen type II. Bioassay and subsequent western blot showed that PTE significantly inhibited the activation of PI3K/AKT and NF-κB signaling pathways. The results of molecular docking experiments showed that PTE could bind closely to the sites of PI3K protein, thereby inhibiting the phosphorylation of PI3K. Conclusions: The experimental results indicate that PTE plays an anti-chondrocyte senescence role in the treatment of OA by inhibiting the PI3K/AKT/NF-κB signaling pathway and reducing expression of SASP.

Keywords: Osteoarthritis, senescence, pterostilbene, chondrocyte

Introduction

Osteoarthritis (OA) is the most common degenerative joint disorder worldwide, affecting about 80% of people over the age of 65 [1]. OA is the leading cause of disability in the elderly. OA is expected to become the leading cause of disability in humans by 2030 [2]. The loss and degeneration of cartilage are the basic pathologic changes of osteoarthritis, but the occurrence and progression of OA involve articular cartilage, synovial tissue, subchondral bone, and other articular tissues, as well as complex molecular mechanisms, bringing difficulties in the treatment of OA [3]. Many different drugs are used to treat the pain of OA, but none can stop the progression of the disease.

OA can be classified as primary or secondary (secondary to trauma, congenital or acquired joint structural abnormalities, etc.). OA is caused by a variety of risk factors, among which an increase in age has the most prominent influence [4]. With the improvement in living and health conditions, the average life expectancy of humans is increasing year by year, and China has an aging society. In the past few decades, the incidence of OA, one of the age-related diseases, has also increased. Cell senescence is one of the signs of aging. Senescent cells cease cell division and release senescence-related secretory phenotype (SASP), which leads to inflammation and senescence of other cells and damage to issue regeneration, leading to the onset and progression of OA [5]. Targeted therapy of cell aging has gradually become a hot topic in OA treatment in recent years [6].

Long thought of as wear and tear disease, OA is now considered a low-grade inflammatory disease that involves all tissues inside the joint. These pathologic processes include low-level inflammation, significant changes in molecular mechanisms, and the decline of immune system function with aging, and these processes are collectively known as inflammaging [7]. This aseptic inflammation triggers cell senescence, causes irreversible cell cycle arrest, and causes significant phenotypic changes such as the production of biologically active secretory components, known as senescence associated secretory phenotype (SASP). SASP can spread senescence from cell to cell in paracrine form, thus intensifying the pro-senescence effect of senescent cells. SASP secreted by senescent chondrocytes will lead to an imbalance of articular cartilage synthesis and catabolism and eventually lead to structural dysfunction. This process can be enhanced by oxidative stress, mitochondrial dysfunction, genomic damage, or other stressors that induce aging.

SASP is regulated at multiple levels, including transcription, translation, mRNA stability, and secretion. The SASP level also depends on positive feedback loops that are autocrine and paracrine, resulting in a cascade amplification effect. Studies have shown that multiple signaling pathways including DNA damage response (DDR), P38 MAP kinase, and cGAS/STING are involved in the regulation of SASP. These cascades ultimately focus on the activation of NF-κB and CCAAT/enhancer binding protein-β (C/EBPβ) [8]. During the occurrence and development of OA, a complex signaling pathway network mediates pathologic events in chondrocytes, in which NF-κB plays a key role in many pathophysiologic processes of OA and is considered one of the therapeutic targets in OA [9, 10]. NF-κB also plays a key regulatory role in the secretion and expression of SASP [11]. NF-κB is activated and enriched in the chromatin portion of senescent cells and regulates SASP expression by directly controlling the transcription of important inflammatory SASP regulators such as IL-6 or IL-8. In turn, key SASP factors act in an autocrine precursor loop that enhances NF-κB activity and amplifies SASP signaling.

Basic and clinical research on anti-aging therapy have advanced in recent years. Although drugs that selectively kill senescent cells (known as "senolytics") are an attractive approach for anti-aging therapy, regulatory therapies targeting SASP are emerging as another important option for therapeutic strategies targeting aging-related diseases [12]. SASP is closely related to aging and aging-related diseases. Inflammaging is the pathologic basis of many aging-related diseases [13]. SASP can explain, at least to a certain extent, local inflammatory changes in tissues during aging, and OA is no exception, as a typical aging-related disease.

At present, no drug can prevent the onset and progression of OA, so it is an urgent task to find disease-modifying drugs (DMOADs) to reverse OA [14]. Natural extracts have unique advantages such as being anti-inflammatory, antioxidant, and showing low drug toxicity and good tolerance [15, 16]. These are increasingly favored by researchers and clinicians [17]. Recent studies have found that natural extracts play a significant role in the treatment of OA [18-21].

Pterostilbene (PTE) is a trans-stilbene compound. In nature, PTE is widely distributed. Because it was originally found in red sandalwood, it was named pterostilbene. It has a variety of biologic activities such as antioxidant, anti-tumor, hyperemia, and bacteriostasis [22]. PTE has rarely been studied in the treatment of OA, especially its effect on cartilage aging.

In this study, we aimed to examine the therapeutic effects of pterostilbene on articular chondrocyte senescence and OA in vivo and used in vitro experiments to explore the role of NF-κB and its upstream and downstream pathways in the above therapeutic effects of PTE.

Materials and methods

Animals

Male Sprague-Dawley rats were obtained from HFK Bioscience Co. Ltd. (Beijing, China). Rats were housed in cages with a 12 h light-dark cycle, 70% humidity, and 20-25°C ambient temperature. All rats were acclimated for 1 week to adapt to laboratory conditions before experimental procedures. Experiments involving animals should follow the appropriate institution or the National Research Council Guide for the care and use of laboratory animals. All animal experiments were performed following the principles of the Animal Ethics Committee of Shengjing Hospital of China Medical University (2017PS237K, Shenyang, China).

OA model and PTE treatment

As previously mentioned, OA was surgically induced in the right knee by transection of the anterior cruciate ligament (ACLT) and destabilization of the medial meniscus (DMM) [23]. 18 Male Sprague-Dawley (SD) rats (5-weeks-old, 188 ± 5 g) were divided into three groups (n = 6): CG, OA (ACLT+DMM), OA+PTE. The general procedure was as follows: the rats were first anesthetized after intraperitoneal pentobarbital sodium injection (40 mg/kg) and subsequent surgery was performed; then we used microsurgical scissors to cut the ACL and the connection of the medial meniscus to the tibial plateau. In the control group, only the right knee arthrotomy was performed, excluding the surgery of ACLT+DMM.

PTE (20 mg/kg) was intraperitoneally injected into OA+PTE (20 mg/kg) every 3 days from the 3rd day after the surgical modeling, and the drug injection lasted for 5 weeks. The CG group and OA group were injected with equal amounts of DMSO and sterile saline.

Enzyme-linked immunosorbent assay (ELISA) of intra-articular lavage fluid

IL-6 levels in the knee intra-articular lavage fluid were determined using ELISA kits (E-EL-

R0015C; Elabscience; Wuhan, China) following the manufacturer's instructions. Then, the content of protein in intra-articular lavage fluid was measured to ensure that the ratio of dilution was equal.

Histologic and immunohistochemical assessment

Rat knee joint samples were fixed in 4% formaldehyde for 1 week and decalcified with 20% ethylenediaminetetraacetic acid disodium salt (EDTA-2Na) (pH 7.0) solution for 3 weeks. The solution of EDTA-2Na was changed every 3 days. Decalcified samples were dehydrated in graded ethanol, transparentized in dimethylbenzene, and embedded in paraffin. Serial 5-μm sagittal sections were collected for histologic examination. Sections were deparaffinized in xylene and graded alcohol. Serial sections were stained with hematoxylin-eosin and toluidine blue to observe cartilage tissue for immunohistochemical analysis. Enzymatic antigen retrieval reagent was applied to the sections for 30 min at 37°C. Then, the sections were incubated in 3% H_2O_2 for 30 min at 37°C to inhibit endogenous peroxidases. Sections were blocked with goat serum for 30 min at room temperature and incubated overnight with rabbit primary antibodies against collagen type II (1:100; ab34712, Abcam, USA), MMP-13 (1:100; ab39012, Abcam, USA), IL-6 (1:100; A0286, Abclonal, China), p16 (1:50; A0262, ABclonal, China) and p21 (27296-1-Ap, Proteintech, China) at 4°C. Negative control histochemical sections were used PBS instead of primary antibody. Sections were washed three times with PBS and incubated with horseradish peroxidase-conjugated anti-rabbit secondary antibody for 30 min at 37°C. Finally, the sections were stained with a DAB kit (Zhongshan Golden Bridge Biotechnology, China). Images were collected with an Olympus BX53 microscope. The degree of OA was evaluated by two investigators in a blinded manner following Mankin scores and Osteoarthritis Research Society International (OARSI) scores. Image-pro Plus 6.0 software was used for statistical analysis of immunohistochemical images.

Isolation, culture, and identification of primary rat chondrocytes

Primary chondrocytes were obtained from the knee cartilage of male SD rats (4-weeks-old). Cartilage tissue was collected and trimmed to

1 mm^3 in sterile phosphate buffer saline (PBS). Pronase (4 mg/ml; Roche, Switzerland) and collagenase (1.6 mg/ml; Roche, Switzerland) were diluted using serum-free Dulbecco's Modified Eagle Medium/F12 (1:1) (Gibco, USA). Cartilage pieces were first digested with pronase for 2 h at 37°C, cyclically followed by collagenase at 37°C with moderate shaking. Each cycle of collagenase digestion lasted for 40 min. After each digestion cycle, cell suspensions were carefully collected, and centrifuged at 800 rpm for 5 min to separate the cells and collagenase solution. The collagenase solution (i.e. the supernatant) was collected and mixed with the remaining cartilage pieces for the next digestion cycle. Normally, the collagenase digestion lasted for 6 cycles. The collected cells were resuspended and cultured in DMEM/F12 (1:1) supplemented with 10% fetal bovine serum (FB15015, Clark, China), as well as 1% penicillin and streptomycin (Hyclone, USA), at 37°C in a 5% CO_2 incubator. The medium was changed the day after isolation, to remove any dead or unattached cells. Fresh medium was added every 3 days. Cells were passaged in a 1:3 ratio after reaching 70%-80% confluence. After 2 passages, the cells were used for experiments. Collagen type II immunofluorescence was used to identify chondrocytes.

Cell viability and cytoxicity assays (MTS)

Cytotoxicity test of PTE was performed using the MTS method according to the instructions (Abcam, ab197010, USA). The absorbance value was read at 492 nm after incubation at 5% CO_2 and 37°C for 1 h.

Treatment with IL-1β and PTE

Cell group A: control group (CG); B: IL-1β; C: IL-1β+10 µmol/L PTE; D: IL-1β+20 µmol/L PTE. In vitro chondrocyte senescence was induced by 24-h IL-1β (MCE, HY-P7097, USA) stimulation of normal chondrocytes. The simulated inflammatory OA environment under the treatment of IL-1β can also induce chondrocyte senescence.

Senescence-associated β-galactosidase (SA-β-Gal) assay

The SA-β-Gal activity was measured using a staining assay (Beyotime, Jiangsu, China) according to the manufacturer's protocols. The percentage of SA-β-Gal-positive cells from three random fields was quantified.

Flow cytometric cell cycle analysis

After modeling, chondrocytes in each experimental group were washed once with PBS and centrifuged at 1500 rpm for 5 min. Cell concentration was adjusted to 1×10^6/ml, and 1 ml of single-cell suspension was taken. After centrifugation, the prepared single cell suspension was removed from the supernatant, and the cells were fixed with 500 µl 70% precooled ethanol at 4°C for 2 h. Suspension was washed with PBS before staining. 100 µl RNaseA solution was added to the cell precipitate, placed in a water bath at 37°C for 30 min, and then cells were suspended again. 400 µl PI staining solution was added, mixed well, and incubated at 4°C for 30 min away from light. Finally, the cell cycle of chondrocytes in each group was detected by computer, and red fluorescence at the excitation wavelength of 488 nm was recorded.

qRT-PCR

Total RNA from chondrocytes was extracted with RNA isolater Total RNA Extraction Reagent Isolater (TRIzol method, st-795s; beyotime, China). cDNA was reverse transcribed using Hiscript II Q RT Supermix from 1 µg total RNA. Then, qPCR was performed and relative expression was calculated using the $2^{-\Delta\Delta CT}$ method. The primer sequences used for PCR were listed below: β-Actin (F): 5'-CACCCGCG AGTACAACCT-TC-3', (R): 3'-CCACACTACCACCCATACCC-5'; collagen type II (F): 5'-CACTGTAAGAACAGCA TTG-CCTAC-3', (R): 3'-TGAGGTCTTCTGTGATCGGTAC-TC-5'; MMP-13 (F): 5'-ACAGTTGACAGGCTCCG-AGAAATG-3', (R): 3'-CCACATCAGGCACT CCACAT-CTTG-5'; IL-6 (F): 5'-GCCACTGCCTTCCCTACT-TC-3', (R): 3'-GCCATTGCACA ACTCTTTTCTC-5'; p16 (F): 5'-CAAGAGCGGGGACATCAAGACATC-3', (R): 3'-CACAAAGACCACCCAG CGGAAC-5'; p21 (F): 5'-TAGAACAGTAGACACGAAACAGGC-3', (R): 3'-TCCCATCTTT GCTCATCTTTTC-5'.

Western blot

Cells were lysed in radioimmunoprecipitation assay buffer (RIPA) buffer (Beyotime, China) containing 1 mM phenylmethylsulphonyl fluoride (PMSF) (Beyotime, China) and phosphatase inhibitor (Beyotime, China). Lysates were

centrifuged at 14,000×g for 5 min at 4°C and the supernatants were collected. Protein concentration was measured using the bicinchoninic acid assay (BCA Protein Assay Kit, Beyotime, China) following the manufacturer's instructions. Then, 20 mg of protein, from each lysate, was separated using SDS-PAGE and transferred to a polyvinylidene difluoride (PVDF) membrane. The PVDF membranes were blocked with 5% non-fat milk for 2 h at room temperature and incubated with rabbit polyclonal anti-β-actin (1:1000; WL01372; Wanlei, China), GAPDH (1:1000; 60004-1-Ig; Proteintech, China), rabbit polyclonal anti-collagen type II (1:1000; ab34712, Abcam, USA), rabbit polyclonal anti-MMP-13 (1:3000; ab39012; Abcam, USA), rabbit polyclonal anti-ADAMTS-5 (1:1000; ab41037; Abcam, USA), rabbit polyclonal anti-IL-6 (1:3000; A0286; Abclonal, China), rabbit polyclonal anti-p16 (1:3000; A0262; Abclonal, China), rabbit polyclonal anti-p21 (1:3000; 27296-1-Ap; Proteintech, China), rabbit polyclonal anti-NF-κB p65 (1:3000; A2547; ABclonal, China), rabbit polyclonal anti-p-p65 (1:3000; 3033; CST, USA), rabbit polyclonal anti-PI3K (1:3000; ab 278545; Abcam, USA), rabbit polyclonal anti-p-PI3K (1:3000; AF3241; Affinity, China), rabbit polyclonal anti-AKT (1:1000; WL0003; Wanlei, China), rabbit polyclonal anti-p-AKT (1:1000; WLP001; Wanlei, China), rabbit polyclonal anti-IκBα (1:1000; WL01936; Wanlei, China), rabbit polyclonal anti-p-IκBα (1:1000; WL01936; Wanlei, China) antibodies at 4°C overnight. The Antibodies had been diluted with tris-buffered saline containing Tween-20 (TBST). After three 10-min washes with TBST, the membranes were incubated with horseradish peroxidase-conjugated anti-rabbit secondary antibodies (1:10000; Zhongshan Golden Bridge, Beijing, China), After three washes with TBST, membranes were analyzed via chemiluminescence (Wanlei, China) in an Amersham imager 600 (GE, USA) and quantified using Image J (Ver 1.47, National Institutes of Health, USA). β-actin and GAPDH were used as internal control.

Bioinformatic analysis

Four data sets, GSE55235 (platform file: GPL96, containing 10 normal bone and joint samples and 10 OA samples), GSE55584 (platform file: GPL570, containing 6 OA samples), were downloaded from the NCBI-Geo website (home-GED-NCBI (nih.gov). GSE82107 (platform file is GPL570, which contains 7 normal bone and joint samples and 10 OA samples). The "LIMMA" and "SVA" packages in R (4.0.3) are used for data collation and batch correction. We conducted screening for differentially expressed genes and related signaling pathways in OA and aging pathology. C-map, LINCS, CLUE and CPDB libraries were used to predict the mechanism of PTE's therapeutic role in OA. The size of each point indicates the number of gene entities in the pathway. The line between the two points was calculated based on the function of the two pathways to indicate the number of genes in the overlapping pathways. The width of the line indicates the strength of the correlation between the two points.

Analysis of immunofluorescence

The chondrocytes were rinsed with PBST and treated with 4% paraformaldehyde for 20 minutes. After fixation, we washed with PBST three times for 1 min each. Then 0.5% Triton X-100 was added to break the cell membrane for 10 min. Next, chondrocytes were blocked with 10% goat serum and incubated with primary antibodies against collagen type II (1:300) and NF-κB p65 (1:50) at 4°C overnight. The next day, a fluorescent secondary antibody (1:1000) was added and incubated for 30 min in a dark environment. Finally, DAPI staining was carried out at room temperature for 5 min, and PBST was added and cleaned three times for 1 min each. After all the operations were completed, the tablets were sealed with liquid and stored at -20°C. The images were collected under a fluorescence microscope.

Molecular modeling

First, we mapped the molecular structure of DE using ChemBioDraw and used ChemBio3D to minimize its energy. According to the needs of current molecular docking experiments, we downloaded the corresponding PI3K (PDB code 5IS5) from the PDB website (https://www.rcsb.org/). After being treated by PyMoL (version 1.7.6), the lowest energy conformations for docking were decided by default values. When the molecular structure of DE and PI3K required for docking analysis was ready, subsequent molecular docking was started. The docking analysis was performed by AutoDockTools (version 1.5.6). The eventual pictures of 3D views were performed using the PyMoL.

Statistical analysis

All experimental data were repeated 3 times, expressed as mean ± standard deviation. SPSS and GraphPad Prism software were used for the statistical analysis of data. Shapiro-Wilk and Levene tests were used to verify whether the data conformed to normal distribution and homogeneity of variance. If the data were consistent, one-way ANOVA was used. If the data did not meet the normal distribution, the rank sum test was used. For data comparison, $P < 0.05$ was considered significant (*: $P < 0.05$, **: $P < 0.01$, ***: $P < 0.001$, ****: $P < 0.0001$).

Results

Histopathologic evaluation of knee joints of rats in each group

In the control group (CG), the surface of knee cartilage was intact without cartilage damage. In ACLT+DMM induced OA model group, the surface of articular cartilage was uneven and toluidine blue staining was uneven. PTE showed a good therapeutic effect on OA. Mankin scores and OARSI scores of knee joints of rats in each group showed that after 6 weeks of ACLT+DMM modeling, the knee joints of rats showed signs of mid-early osteoarthritis, while after PTE treatment, the Mankin scores and OARSI scores of knee joints of rats decreased significantly (**Figure 1**).

Immunohistochemical results of knee cartilage of rats in each group

Compared to the CG group, chondrocytes with positive expression of collagen type II (COL2) were significantly decreased in the OA group, and the chondrocytes with positive expression of MMP-13 and IL-6 were significantly increased. The positive expression of two major markers of aging, p16 and p21, also increased significantly. Compared to the OA group, chondrocytes expressing collagen type II (COL2) were increased in the OA+PTE group, while the number of MMP-13 and IL-6 positive chondrocytes was significantly decreased. Chondrocytes with positive expression of senescence related markers p16 and p21 were also significantly reduced (**Figure 2**). The correlation between aging markers and OA severity in rats showed that the rate of chondrocytes with p16 and p21 positive expression was significantly positively correlated with Mankin scores and OARSI scores (Figure S1).

ELISA detection of joint cavity lavage fluid

Compared to the CG group, IL-6 content in knee lavage fluid of ACLT+DMM rats 6 weeks after modeling was significantly increased. At the same time, the level of IL-6 in knee lavage fluid in OA+PTE group was significantly lower than that in OA group (**Figure 2G**).

Identification of primary chondrocytes in rats

The primary chondrocytes extracted from the articular cartilage of the rat knee joint were observed under a confocal microscope in polygonal shape (**Figure 3A**) and gradually changed into a long spindle shape after passing for 3 generations at a ratio of 1:5. Due to the need to maintain chondrocyte consistency to control variables, chondrocytes less than the second generation were used for follow-up experiments in this study.

MTS assay

The effects of PTE (**Figure 3E**) at 5 concentration gradients (10, 20, 40, 60, 80 μmol/L) on the cell viability of rat chondrocytes were detected in MTS experiment (24 h, 48 h), and the results showed that there was no significant difference in the cell viability of chondrocytes in each group compared with the blank group. Finally, 10 μmol/L and 20 μmol/L (24 h) were selected as drug concentrations for subsequent experiments (**Figure 3B**).

SA-β-Gal staining

Compared with the control group, IL-1β (10 ng/mL) could induce chondrocyte senescence significantly, and the ratio of SA-β-Gal staining positive cells was significantly increased. PTE significantly reduced the ratio of SA-β-Gal positive chondrocytes in a concentration-dependent manner, and the effect of 20 μmol/L PTE was significant compared to 10 μmol/L (**Figure 3C**, **3D**).

Cell cycle

Cell cycle test results (**Figure 4**) showed that inflammatory induction of IL-1β (10 ng/mL) significantly increased the proportion of chondrocytes in G0-G1 phase compared with the con-
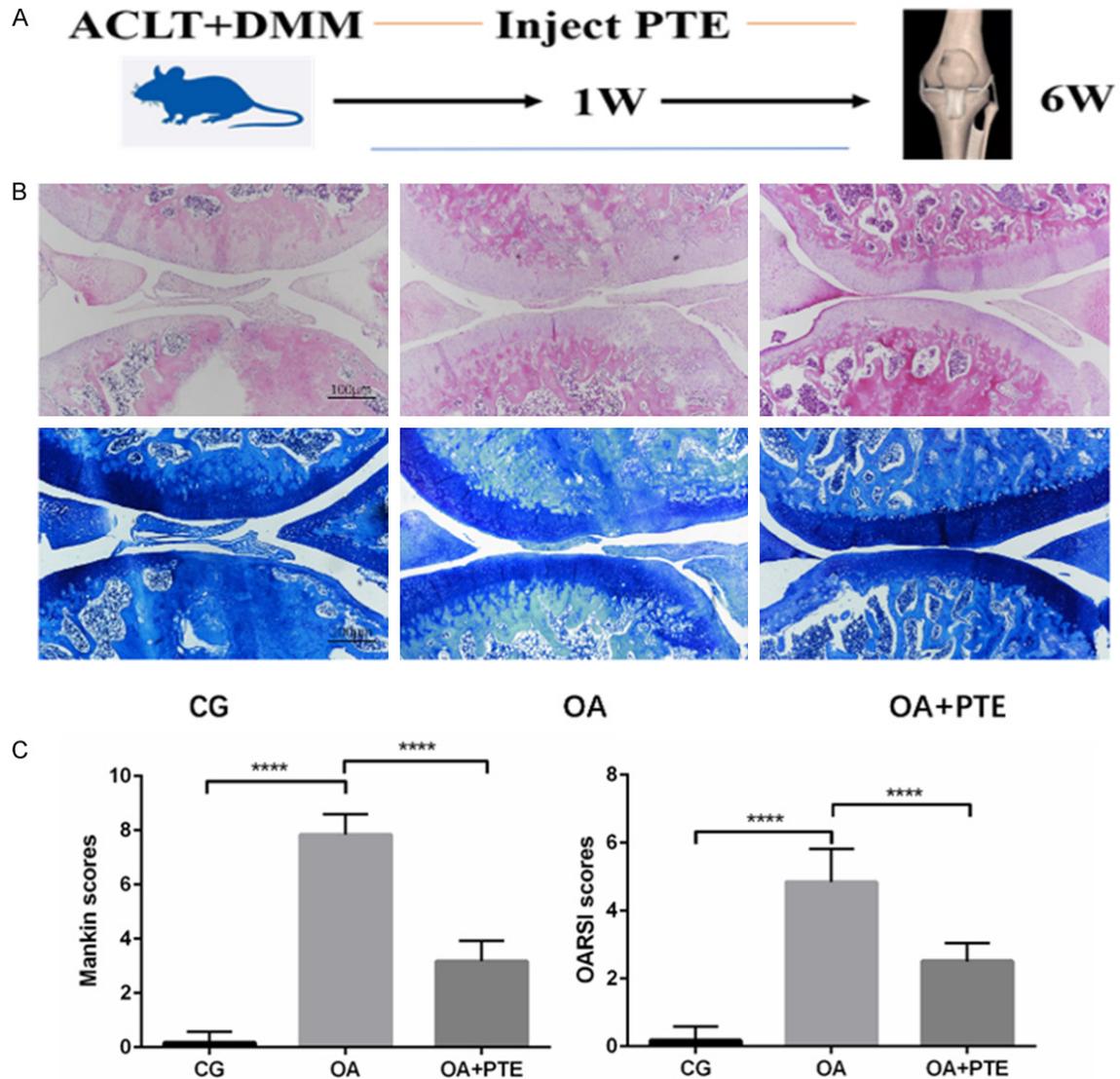
Figure 1. A. Time axis of rat modeling and PTE administration. B. The results of H&E and toluidine blue staining in pathologic examination of knee joints of rats in each group. C. The results showed that Mankin score and OARSI score were significantly increased after ACLT+DMM modeling, which induced the occurrence of osteoarthritis in the middle and early stage of the knee in rats, while PTE could significantly reduce OA severity scores. *: P < 0.05, **: P < 0.01, ***: P < 0.001, ****: P < 0.0001.

trol group, leading to cell cycle arrest, a hallmark of senescent cells. However, the proportion of G0-G1 cells in the two PTE treatment groups was significantly reduced, indicating that PTE treatment reduced the degree of chondrocyte cycle arrest, reflecting a decrease in cell senescence.

qRT-PCR

PCR was used to verify the therapeutic effect of PTE. Results showed that IL-1β significantly increased the expression of MMP-13, IL-6, P16

and P21, and significantly decreased the expression of type II collagen (COL2), which could be inhibited by PTE, with significant differences (**Figure 5**).

Western blot

Western Blot results (**Figure 6**) showed that 10 ng/mL IL-1β significantly induced inflammatory response of chondrocytes, specifically, significantly increased the expression of ADAMTS-5, MMP-13 and IL-6, and decreased the expression of type II collagen. IL-1β induced chondro-
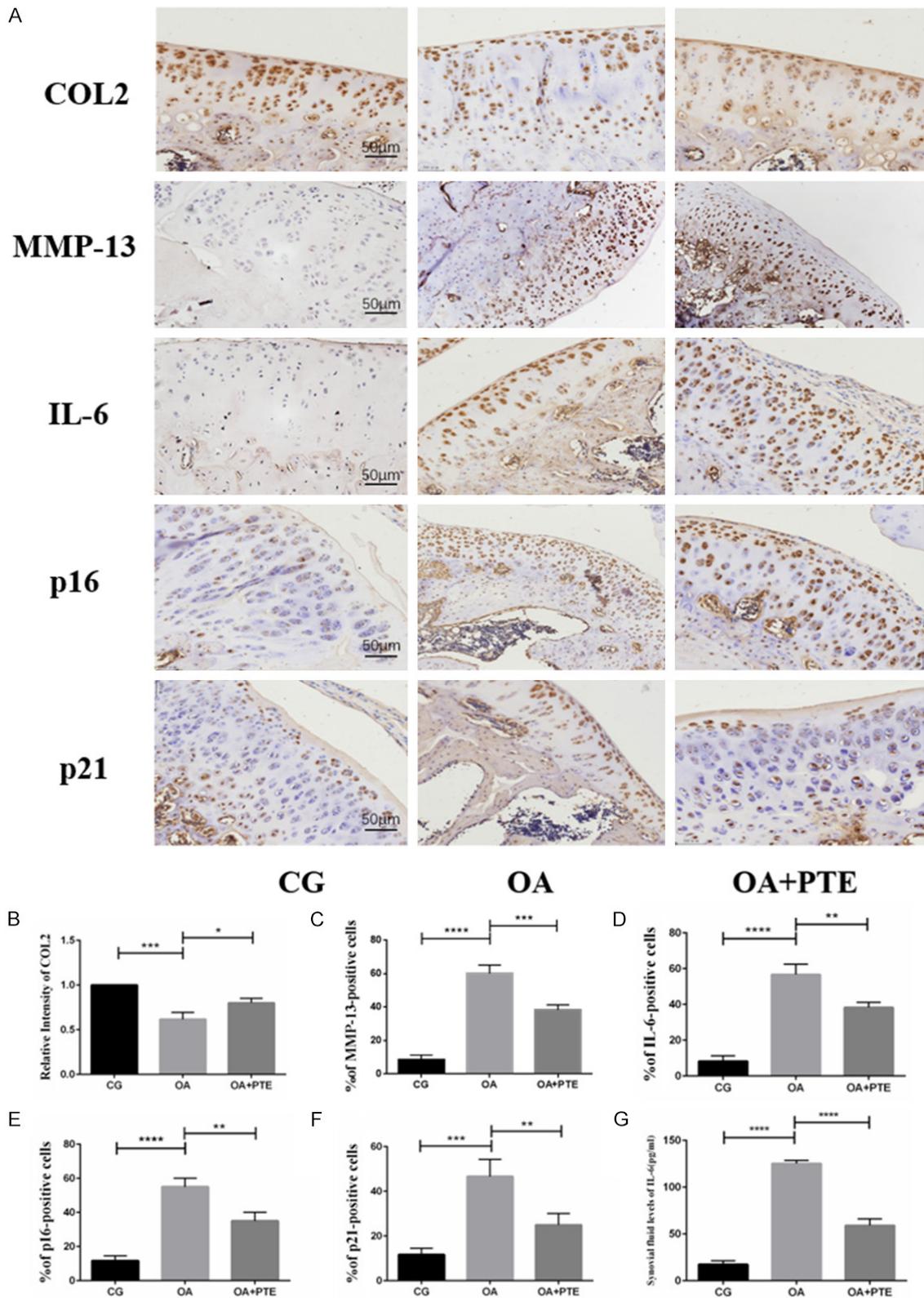
Figure 2. A. Immunohistochemical results on knee joints of rats in each group. B-F. The results showed that the expression of type II collagen (COL2) decreased after ACLT+DMM modeling, while the expression levels of MMP-13 and IL-6 positive cells increased, and the expression levels of p16 and P21 positive cells also significantly increased. After the application of PTE, the expression of type II collagen was increased, and the expression levels of MMP-13, IL-6, P16, and P21 positive cells were also significantly decreased. These results indicate that PTE has anti-inflammatory and anti-aging effects in OA model rats. G. Elisa *: $P < 0.05$, **: $P < 0.01$, ***: $P < 0.001$, ****: $P < 0.0001$.
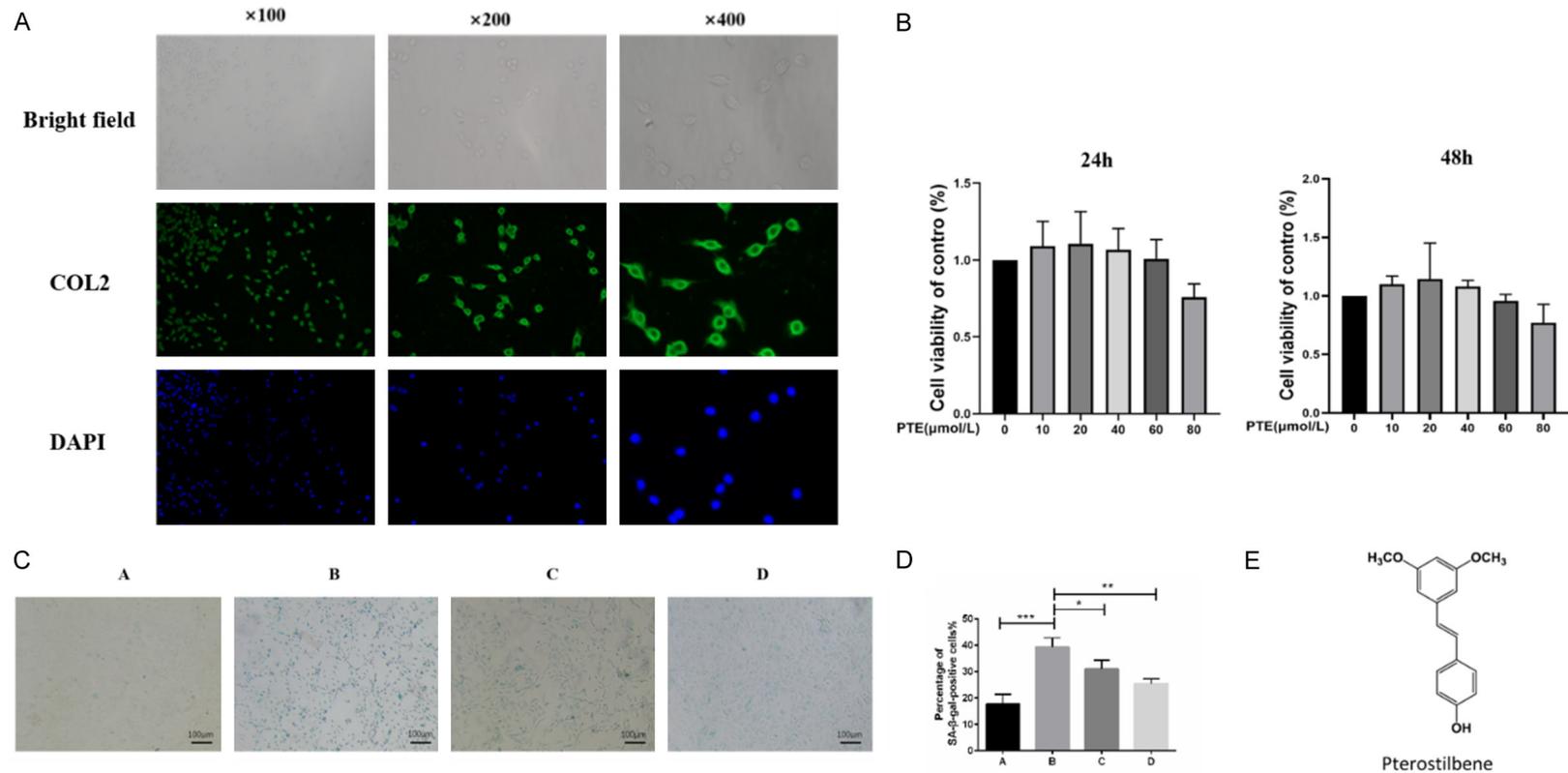
Figure 3. A. The chondrocytes were identified by immunofluorescence staining of type II collagen. Under a confocal microscope, the extracted cells were polygons with strong fluorescence signal of type II collagen, so the extracted cells were identified as chondrocytes. B. MTS cell viability test (24 h, 48 h). C. SA-β-Gal staining (ratio: 100×). Group A: CG; B; Il-1 β (10 ng/ mL); C: IL-1β+PTE (10 μmol/L); D: IL-1β+PTE (20 μmol/L). D. The blue staining results of SA-β-Gal staining showed senescent chondrocytes, and IL-1β could significantly induce senescence of chondrocytes. PTE decreased the ratio of SA-β-Gal positive cells, and 20 μmol/L PTE inhibited chondrocyte senescence significantly compared with 10 μmol/L PTE. E. Molecular structure of PTE. *: P < 0.05, **: P < 0.01, ***: P < 0.001.
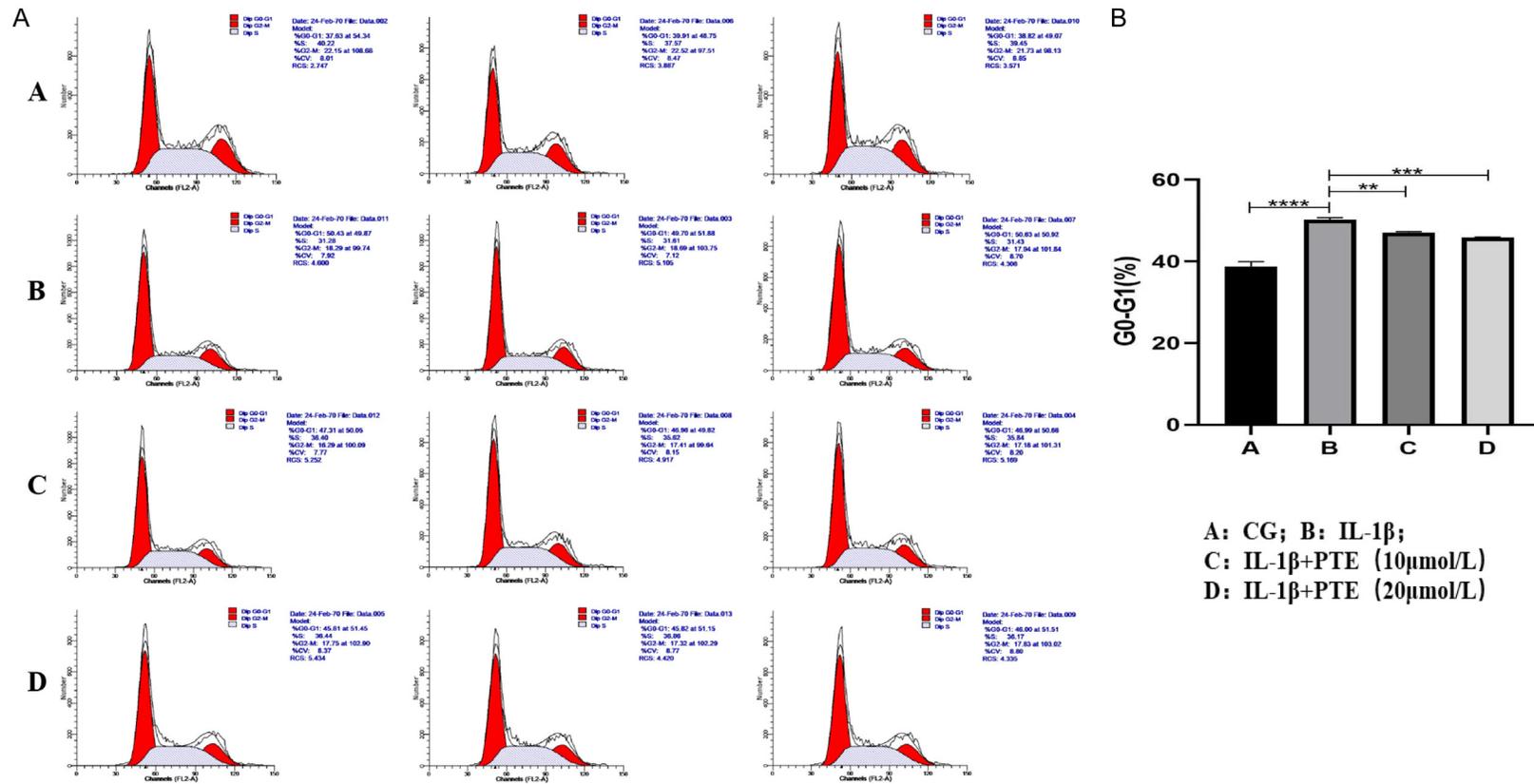
Figure 4. A, B. Cell cycle results, group A: CG; B; Il-1 β (10 ng/ mL); C: IL-1β+PTE (10 μmol/L); D: IL-1β+PTE (20 μmol/L), the experimental results were repeated three times. The proportion of G0-G1 chondrocytes in group B (IL-1β group) was significantly increased, while G0-G1 chondrocytes in PTE group were significantly decreased. *: P < 0.05, **: P < 0.01, ***: P < 0.001, ****: P < 0.0001.
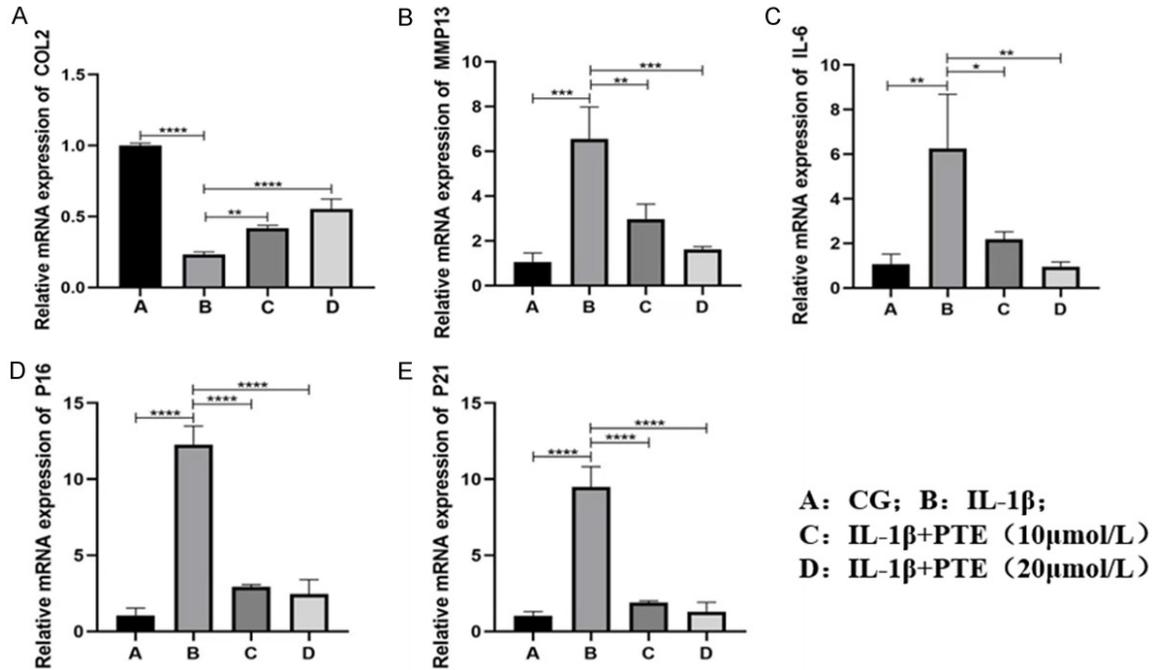
Figure 5. A-E. mRNA changes of genes related to inflammation and aging induced by IL-1β inflammation. Data are shown as the mean ± standard deviation, n = 3; A: CG. B: IL-1 beta; C: IL-1β+PTE (10 μmol/L); D: IL-1β+PTE (20 μmol/L). *: P < 0.05, **: P < 0.01, ***: P < 0.001, ****: P < 0.0001.

cyte senescence, and the expression of senescence markers P16 and P21 increased significantly. These pro-inflammatory and pro-aging effects of IL-1β could be inhibited by PTE, and the anti-inflammatory and anti-aging effects of 20 μmol/L PTE were more significant than those of 10 μmol/L PTE.

Western blot showed (**Figure 7**) that IL-1β significantly activated PI3K/AKT and NF-κB signaling pathway, and the ratio of P-PI3K/PI3K, P-Akt/AKT, P-P65/P65 and the expression of P-I κBα were significantly increased compared with the control group in the subsequent study on mechanism. However, PTE at 10 μmol/L and 20 μmol/L significantly inhibited the activation of PI3K/AKT and NF-κB signaling pathways.

Bioinformatic analysis

We obtained 27 normal tissue microarray results and 36 OA tissue microarray sequencing results. The results of differential analysis were obtained by using "GGplot2" package, "Limma" package and "Pheatmap" package in R, and the volcano map and heatmap were plotted (logFC > 1, P < 0.05 as screening conditions). A total of 219 differential genes were

obtained. We further use the "Clusterprofiler", "enrichPlot", "org.hs.eg.db" and "GGploT2" packages for GO and KEGG enrichment analysis and to plot bar and bubble charts. At the same time, differential genes were introduced into Metascape for GO and KEGG enrichment and protein interaction network mapping. The results showed that NF-κB signaling pathway plays an important role in OA, and NF-κB also regulates SASP expression and plays a key role in the pathological process of aging. Differentially expressed MMP-13 and IL-6 in OA are also important members of SASP and are regulated by NF-κB. The PI3K/AKT signaling pathway, which also plays an important role in OA, was shown to be an upstream signaling pathway of NF-κB in bioassay results. We used C-map, LINCS, CLUE and CPDB libraries to predict the mechanism of PTE's anti-inflammatory effect on aging in OA. The network showed a correlation between NF-κB signaling, aging and autophagy. Pathway analysis of Kyoto gene and KEGG also showed that NF-κB pathway is involved in the regulation of cell senescence and is an important pathway in cell senescence. CELLULAR SENESCENCE was searched through KEGG PATHWAY database (Genome. JP), and the results also showed that NF-κB
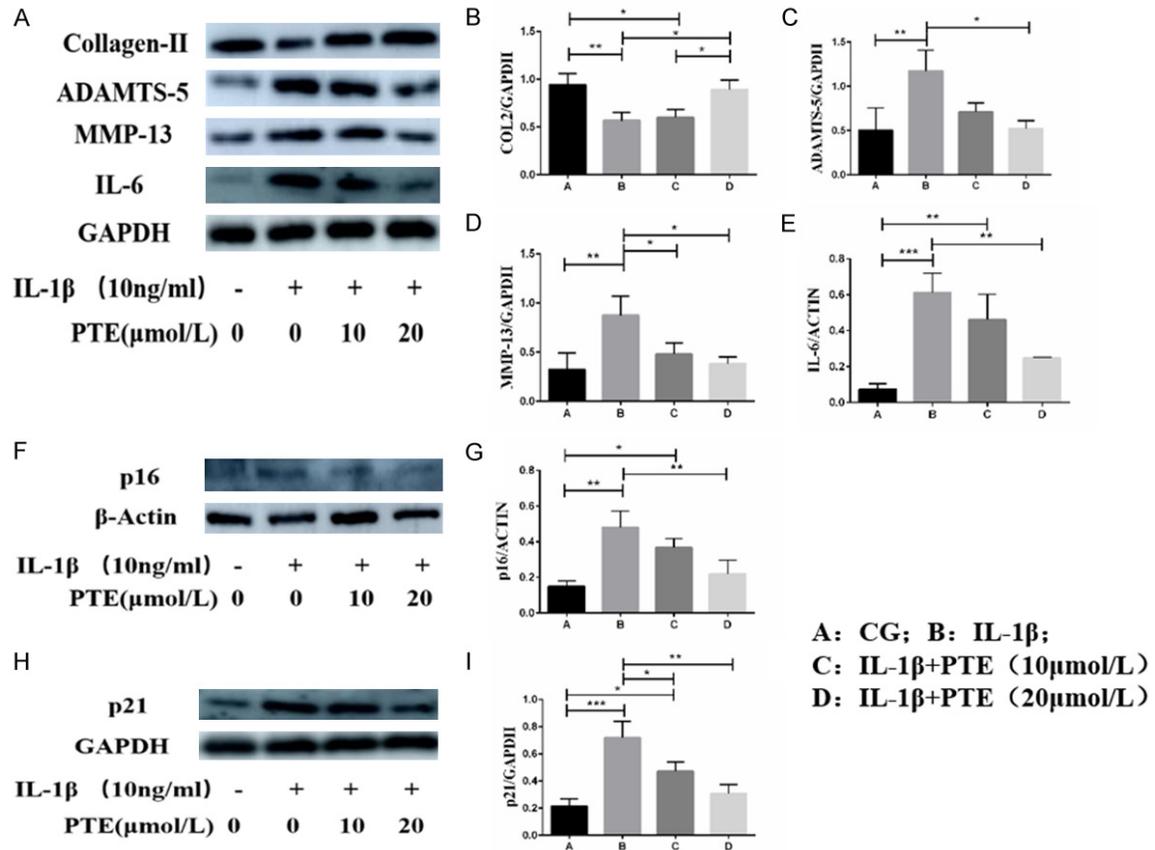
Figure 6. A-I. Western blot was used to detect the protein expression levels of type II collagen (COL2), ADAMTS-5, MMP-13, IL-6, P16 and P21. Data are shown as the mean ± standard deviation, n = 3. *: P < 0.05, **: P < 0.01, ***: P < 0.001.

pathway was involved in regulating cell senescence (Figure S2).

Immunofluorescence

We used immunofluorescence to investigate the nuclear translocation of NF-κB P65 in chondrocytes in response to IL-1β-induced inflammation. As shown in **Figures 3** and **4**, most P65 is present in the cytoplasm of the control group and is shown to be nucleonuclear after IL-1β inflammatory stimulation. PTE blocks this expression and retransfers P65 to chondrocyte cytoplasm. These results suggest that PTE plays an anti-inflammatory and anti-aging role by inhibiting nuclear NF-κB P65 translocation (**Figure 8A**).

Molecular docking

Whether PTE directly interacts with PI3K, an upstream protein of the PI3K/AKT/NF-κB pathway, was determined by molecular docking technique. Ten different conformations can be

obtained from one docking result. The conformation with the minimum binding energy (Binding energy = -6.89 kcal/mol) was selected as the optimal binding conformation. In the figure, the macro and local effects of the interaction between PTE and PI3K protein residues are represented by the Ribbon model. The spatial filling model visually displays the spatial position of PTE combined with PI3K (**Figure 8B**). Through the analysis of molecular docking studies, we found that there were important hydrogen bonds in the molecular structure of PTE bound to the amino acid residues of PI3K (Glu-628, ASP-584, ARG-389). Thus, PTE can inhibit SASP expression by regulating PI3K/ AKT/NF-κB signaling axis and play an anti-inflammatory and anti-aging role in OA treatment (**Figure 9**).

Discussion

In this study, using in vivo experiments, we performed transection of the anterior cruciate ligament and destabilization of the medial menis-
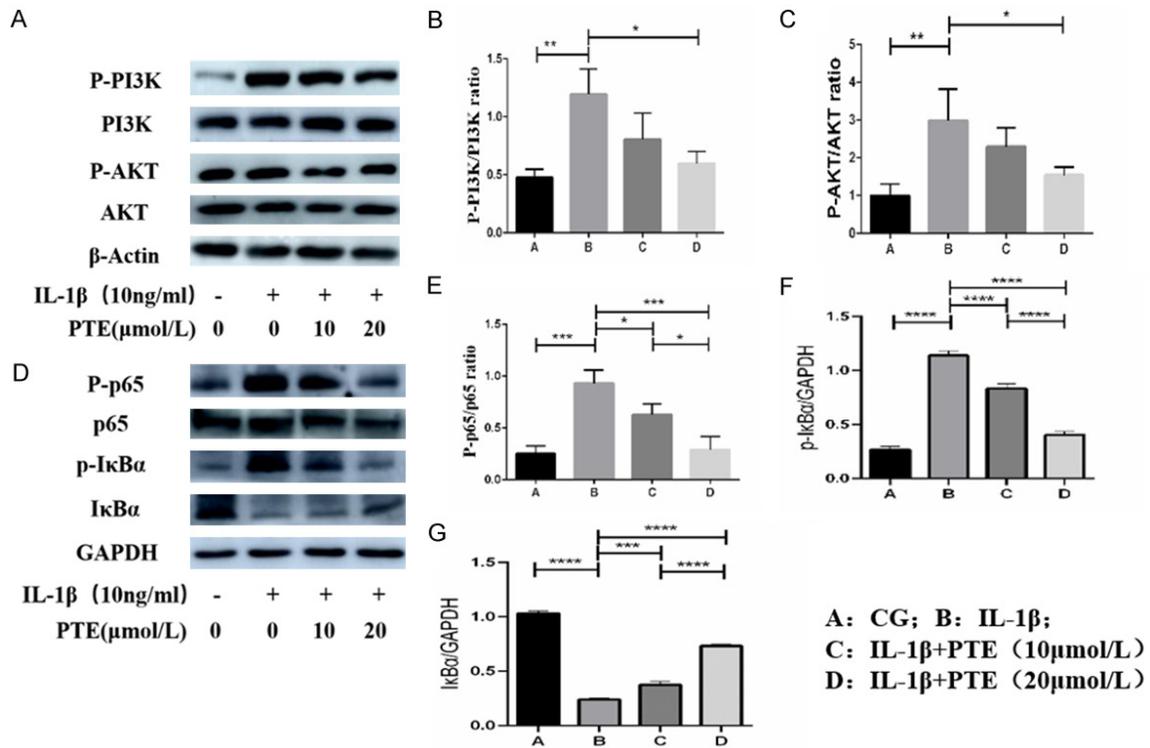
Figure 7. A-G. The expression of related proteins in PI3K/AKT/NF-κB signaling pathway was detected by western blot. IL-1β significantly activated PI3K/AKT/NF-κB signaling pathway, while PTE inhibited the activation of PI3K/AKT/NF-κB signaling pathway. Data are shown as the mean ± standard deviation, n = 3. *: P < 0.05, **: P < 0.01, ***: P < 0.001, ****: P < 0.0001.
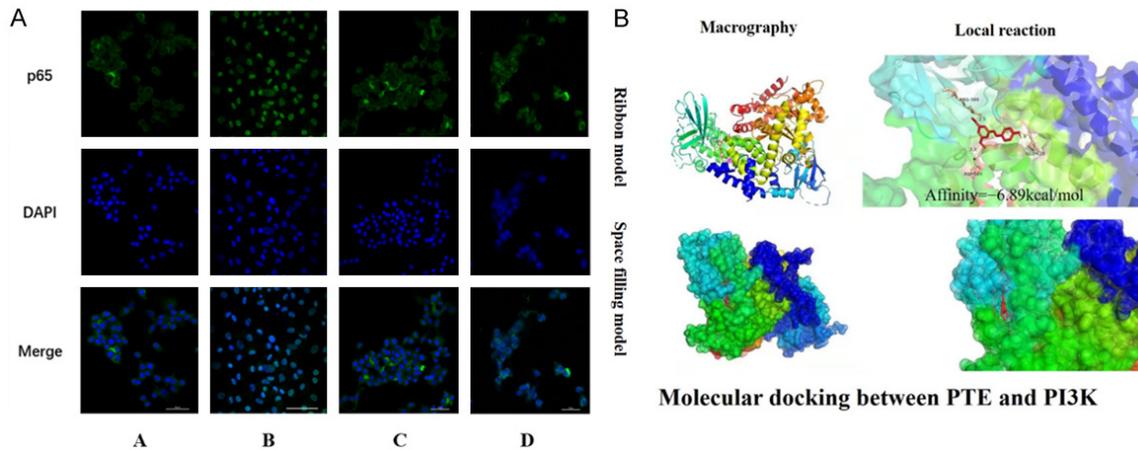
Figure 8. A. Immunofluorescence showed that IL-1β inflammation induced nuclear inward migration of P65, and p65 was re-transferred to chondrocyte cytoplasm under PTE. These results suggest that PTE can play an anti-inflammatory and anti-aging role by inhibiting nuclear translocation of P65. Group A: CG; B; IL-1β (10 ng/ mL); C: IL-1β+PTE (10 μmol/L); D: IL-1β+PTE (20 μmol/L). B. Molecular docking results showed that PTE could stably bind to the amino acid residues of PI3K (Glu-628, ASP-584, ARG-389) and play a role in inhibiting the activation of PI3K, with a binding energy of -6.89 kcal/mol.

cus in SD rats to induce an animal model of knee osteoarthritis. This OA model is simple, safe, and reliable in actual operation [24]. No

antibiotics were used after the operation, and no complications such as incision infection, poor healing, or even postoperative death
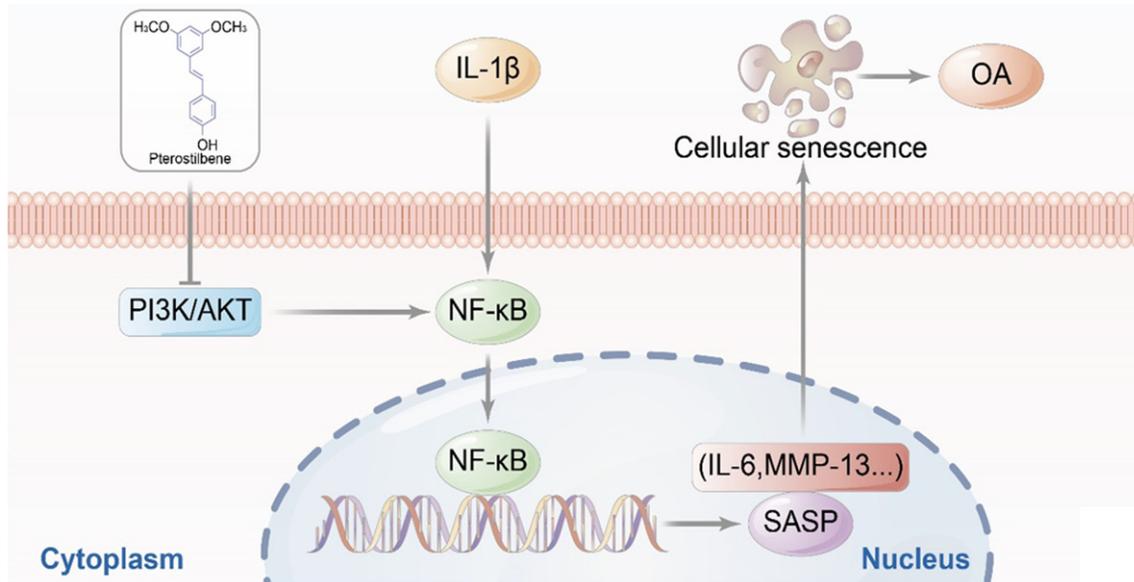
Figure 9. Mechanism of PTE against chondrocyte senescence and OA.

occurred. The use of ACLT+DMM in rats and mice to induce knee OA is now a common method in animal experimental studies of osteoarthritis [25]. This modeling method well simulates the pathophysiologic characteristics of human OA and is widely used in studies on the pathogenesis and drug efficacy of OA [26]. According to previous literature reports, this surgical method can induce knee OA 4 weeks after modeling in mice, and moderate to severe OA 8 weeks later [27]. In this study, 6 weeks after the rat model was established, the articular cartilage of the knee joint of rats in the OA group showed the manifestations of early osteoarthritis, and the immunohistochemical results showed the expressions of type II collagen and MMP-13 were significantly increased. The Mankin scores and OARSI scores in the OA group were significantly higher than those of the control group. The scoring system for cartilage degeneration proposed by Mankin et al. has been applied for more than 40 years and is the most commonly used histologic scoring system in OA research. The OARSI scoring system, however, was proposed in 2006. OARSI scoring is characterized by being able to identify differential changes in early or mild OA [28]. Previous studies have confirmed a good correlation between the Mankin scoring system and the OARSI scoring system. After PTE treatment, OA severity in knee cartilage was significantly reduced after ACLT+DMM modeling, and

Mankin and OARSI histological scores were significantly reduced, indicating that PTE has therapeutic value for OA.

We used IL-1β to induce rat chondrocytes to simulate the OA inflammatory model. Il-1 β is a commonly used drug to simulate the inflammatory environment of osteoarthritis in vitro studies and is considered to be a key regulator of cartilage catabolic metabolism [29]. The IL-1 superfamily consists of 11 members, including 7 receptor agonists (IL-1α, IL-1β, IL-18, IL-33, IL-36 IL-1α, IL-36β, and IL-36γ). Three of these had antagonistic activity (IL-1RA, IL-36RA and IL-38) and one anti-inflammatory cytokine (IL-37). IL-1β, first discovered in the IL-1 superfamily, is one of the most important cytokines promoting inflammation and catabolic metabolism in the pathophysiology of OA. It plays a significant catabolic role in cartilage by increasing the expression and activity of key matrix-degrading enzymes. In addition, IL-1β reduces the synthesis of key extracellular cartilage matrix components, such as type II collagen and proteoglycans [30]. IL-1β can also induce chondrocyte senescence [31].

In this study, IL-1β increased the ratio of SA-β-Gal positive cells in chondrocytes and induced chondrocyte senescence in vitro. Inflammatory induction of IL-1β also significantly increased the proportion of G0-G1 phase cells in chondrocytes, leading to cell cycle arrest, a landmark

event of senescent cells. Western blot was used to detect the expression of MMP-13, ADAMTS-5, and cartilage degradation enzymes in the inflammatory model group significantly increased, while the expression of type II collagen significantly decreased. IL-1β also increased the expression of other markers of aging, such as IL-6, p16 and p21. After PTE was applied, the pro-inflammatory and pro-aging effect of IL-1β was significantly inhibited, the proportion of G0-G1 chondrocytes was significantly decreased, and the expression of various aging markers was also significantly decreased. The inhibition and treatment effect of PTE on the pathologic process of chondrocyte inflammation and aging was consistent with results of the animal experiments.

Senescence related β-galactosidase (SA-β-Gal) is one of the first described biomarkers. This lysosomal enzyme can be detected by histochemical staining in most senescent cells, but not in non-senescent, quiescent, and immortalized cells. The expression of SA-β-Gal in the articular cartilage of knee OA is closely related to the severity of the disease [32].

One of the main characteristics of senescent cells is that they undergo continuous cell cycle arrest [33]. Unlike quiescent cells, senescent cells are not sensitive to mitotic or growth factor stimulation and cannot re-enter the cell cycle even under favorable growth conditions. Senescent cells also differ from terminally differentiated cells, although terminally differentiated cells are also irreversibly removed from the cell cycle. Terminal differentiation is a defined cell development process that converts undifferentiated precursor cells into specialized effector cells, but cell senescence is primarily a response to cellular stress. The cell cycle is divided into early (G1), S, late (G2) and M stages of DNA synthesis. The regulation of the cell cycle is mainly realized by the arrest of the G1 phase, in which the concept of G0 phase cells came into being. The phase G0 refers to the state of cell stagnation. G0 phase cells break away from the cell cycle and stop cell division, but can enter the cell cycle again under certain conditions of stimulation. Cell senescence, as a protective mechanism, is characterized by permanent arrest of growth, cell cycle stagnation in G1 phase, in order to maintain homeostasis and avoid the transmis-

sion of abnormal genes to the next generation of cells. Therefore, researchers use the ratio of G0 phase to G1 phase as an indicator to identify the degree of cell senescence and the effect of anti-aging treatment [34].

Cellular senescence is a continuous state of cell cycle arrest caused by various stimuli. Senescent chondrocytes are similar in mechanism to other senescent cells, and the key pathways involved in chondrocyte senescence are p16/Rb and p53/p21 pathways. p16 and p21, two cyclin-dependent kinase inhibitors, are components of tumor suppressor signaling pathways regulated by RB and p53 and accumulate in senescent cells. Because the expression of p16 and p21 is closely associated with aging-related cell cycle arrest, they are used as markers to identify senescent cells in tissues and cells in culture. The up-regulation of p16 by various stress responses inhibits the expression of cyclin-dependent kinases (CDKs), reduces the phosphorylation and inactivation of retinoblastoma protein (pRB), and ultimately leads to cell cycle arrest and senescence. In addition, p16 plays an important role in cell cycle regulation by slowing down the process from G1 phase to S phase. p21 is another CDK inhibitor and a major target of p53. Expression of p21 activates p53, which leads to cell growth arrest or apoptosis. The expression of p16 can also reflect the effect of anti-aging therapy with removal of senescent chondrocytes on OA [35]. p16 is thought to be more involved in the maintenance of aging phenotypes, while p21 is key to the establishment of aging [36, 37]. The expression of p16 and p21 in articular cartilage samples of OA patients increased significantly compared with that of healthy controls, indicating the increase of senescent chondrocytes in OA articular cartilage [38]. Other studies have found that SA-β-Gal activity is positively correlated with p16 expression. These two markers were both higher in OA damaged cartilage, suggesting a correlation between aging chondrocytes and OA [39].

Therefore, Gorgoulis et al. proposed the strategy of combining cytoplasmic markers (such as SA-β-Gal), nuclear markers (such as p16, p21), SASP, and other markers to detect senescent cells [40], which has important guiding significance for the identification of senescent chondrocytes and other senescent cells.

The loss of normal function due to aging is related to age-related diseases and tissue degeneration [41]. Aging is a key risk factor for OA, but the clear mechanism of aging and OA development is not completely clear [42]. Aging is one of the research hotspots in OA in recent years [43]. Cellular senescence is one aspect of senescence [44]. Senescent cells accumulate in senescent tissues and lead to the pathologic process of senescence and age-related diseases through various mechanisms [45]. Although senescent cells have stopped cell division, they still have a metabolic function and can secrete a series of SASP. Such as pro-inflammatory cytokines and chemokines, growth factors and matrix metalloproteinases (MMPs), etc. SASP is an important part of this study. SASP has many physiologic functions, such as promoting wound healing, increasing tissue plasticity, and promoting continuous chronic inflammation (known as inflammaging) [46]. The SASP can be considered the "soul" of aging because its secretion is highly active and can change its composition over time. According to the secretion phase, SASP can be divided into early and late SASP. Early SASP is beneficial to the body and can repair damaged tissues by recruiting immune cells (such as macrophages and lymphocytes). At the same time, SASP can stimulate the proliferation and differentiation of adjacent cells to restore the internal stability of tissues. However, if senescent cells cannot be cleared in time and accumulate too much, they will transform into late SASP, which will form a chronic pro-inflammatory microenvironment and promote the emergence of various pathologic states [47]. In recent studies, SASP has been divided into three categories. The first category is the classical SASP. The second type is newly emerged SASP, whose members are extracellular vesicles (EVs), which is called evSASP. The third type is non-classical SASP, including IL-1 receptor (IL-1R), IL-1α [48]. At present, the classic SASP has been more studied. The inflammatory cytokines that can initiate the cascade reaction of cartilage matrix degradation in the progression of OA are also SASP factors, among which MMP-13 is the SASP factor expressed by senescent cells in joints that can play a major role. Il-6 is also one of the most critical members of SASP. In our study, inflammation induced a significant increase in SASP, which promoted the aging process of chondrocytes, accompanied by an increase in senescence related markers.

Bioassay results showed that PI3K/AKT is an upstream signaling pathway that regulates NF-κB, and both of them play important roles in OA. We examined the effects of IL-1β and PTE on the PI3K/AKT/NF-κB signaling pathway, and the expressions of PI3K, P-PI3K, AKT and P-Akt were detected by western blot. The results showed that IL-1β significantly activated the PI3K/AKT signaling pathway and subsequently activated NF-κB. Phosphorylation of PI3K, AKT, and NF-κB P65 was significantly enhanced, and nuclear inward migration occurred in P65, while PTE significantly attenuated these effects of IL-1β on chondrocytes. We then used molecular docking techniques to discover the corresponding sites where PTE binds to the amino acid residues of PI3K. All these indicate that PTE can act on the PI3K/AKT/NF-κB signaling pathway to inhibit SASP, and then inhibit inflammatory aging and treat OA.

NF-κB was discovered in 1986 as a transcription factor specifically binding to the immunoglobulin κ light chain gene enhancer region. Originally thought to be a functional regulator of B cell differentiation, it was later found to be a rapid transcription factor prevalent in eukaryotic cells. NF-κB regulates more than 150 genes, including those involved in physiologic processes such as immunity and inflammation, apoptosis, and cell proliferation. The NF-κB signaling pathway positively regulates genes encoding cytokines such as TNF-α, IL-1β, IL-6, IL-2, and IL-12, and plays an important role in inflammatory responses. A large number of studies have shown that the NF-κB signal in chondrocytes plays a key role in controlling cartilage homeostasis and is closely related to the occurrence and development of OA [49, 50].

Under normal conditions, NF-κB dimer exists in the cytoplasm by binding with IκBα. In response to inflammatory stimulation of IL-1β, phosphorylated IκBα is degraded by protease, resulting in phosphorylation of P65 and subsequent migration of the NF-κB complex into the nucleus. NF-κB activates pro-inflammatory cytokines, resulting in decreased expression of chondrocyte-specific genes (collagen type II, connexin, etc.) and increased expression of MMPs (MMP-1, MMP-3, MMP-13), cytokines (IL-

6, IL-8) and chemokines. In addition, NF-κB production increased with the aging of articular chondrocytes induced by IL-1β stimulation. These negative effects of IL-1β were significantly inhibited by PTE, suggesting that PTE has a protective effect on chondrocytes in the simulated OA environment.

The PI3K/AKT signaling pathway upstream of NF-κB is composed of phosphatidylinositol 3-kinase (PI3K) and protein kinase B (PKB, also known as AKT). PI3K/AKT is an important and very complex signaling pathway that has been identified to impact more than 150 proteins. The activated PI3K/AKT signaling pathway phosphorylates tyrosine residues and provides an anchor site for PI3K binding to membranes that participate in many kinds of extracellular matrix and cytokine signaling. This signaling pathway has many important cell biological functions, such as regulating cell vitality, cell senescence and death. PI3K/AKT activates NF-κB by affecting its upstream IκB kinase. Therefore, activated PI3K and AKT participate in NF-κB P65 phosphorylation and nuclear translocation, promoting the production of inflammatory mediators. The PI3K/AKT signaling pathway is crucial for maintaining healthy homeostasis of joints and is closely related to the pathogenesis of OA [51].

Western blot analysis showed that PTE inhibited PI3K phosphorylation and decreased AKT phosphorylation, thereby decreasing the activity of NF-κB signaling pathway. We used molecular docking in order to understand how PTE interacts with PI3K protein. Molecular docking analysis is often used to explore the interactions between molecules [52]. Docking analysis showed that PTE could stably attach to the PI3K inhibitory binding pocket with high affinity through interaction with amino acid residues (Glu-628, ASP-584, ARG-389). In other words, PTE occupies the binding site and inhibits phosphorylation of PI3K, thereby inhibiting the activation of AKT and its downstream NF-κB signaling pathway. Of course, there may be other mechanisms that have not yet been explored for the therapeutic effect of PTE on OA. Current results suggest that PTE can inhibit the activation of PI3K/AKT/NF-κB signaling pathway by blocking PI3K phosphorylation, and then inhibit the secretion of SASP, thus playing an anti-aging role in OA.

PTE has shown good application prospects and efficacy in the treatment of tumors, diabetes, fatty liver and other diseases [53]. Meanwhile, the role of PTE in prolonging lifespan and anti-aging is gradually attracting people's attention [22]. Xue et al. [54] found that PTE can reduce cartilage degeneration in OA knee model rats and inhibit IL-1β-induced chondrocyte inflammation and ROS production by activating Nrf2 signaling pathway, which is consistent with our research results. As a natural extract, PTE may play a therapeutic role in OA through multiple signaling pathways in chondrocytes. An inhibition experiment of the signaling pathway may better reveal the effect of PTE on inflammation and aging. Further studies on the exact mechanism of PTE and clinical trials are needed, and it may take some time to realize the ultimate application of natural extracts like PTE in clinical OA patients. At the same time, it should be recognized that osteoarthritis is a complex disease involving multiple tissues of the joint, involving multiple biological and mechanical factors, and requires comprehensive treatment. As shown in the experiments in vivo, the application of PTE alone can reduce the severity of OA in model rats, but PTE cannot reverse the condition of OA in rats due to the persistence of knee mechanical instability caused by ACLT and DMM. Aging is a key factor in the pathogenesis of OA. It is believed that anti-aging treatment will become an important part of the comprehensive treatment of OA.

Through in vivo experiments, we used intraperitoneal injection of rats, which has the advantage of simple administration and less stimulation to experimental animals. Intra-articular injection may achieve greater efficacy by targeting avascular cartilage and chondrocytes [55], but requires the operation of anesthetized animals and carries a risk of iatrogenic articular cartilage injury. Since the existence of dense cartilage matrix filled with negatively charged proteoglycan and the rapid metabolism of articular fluid will affect the effect of injecting drugs like PTE into the articular cavity, we will continue to explore appropriate delivery methods of PTE in the future, such as using positively charged drug carriers [56, 57]. Since some SASP members also play important regulatory roles in many other cellular pathways, adverse effects on other physiologic functions should also be considered in SASP inhibition therapy

to minimize side effects while maximizing therapeutic efficacy.

Conclusion

In vivo experiments proved that aging markers were associated with the severity of OA, and PTE could reduce the expression levels of OA inflammation and aging markers, and reduce the severity of OA in knee joints of rats. PTE can also reduce the senescence degree of chondrocytes in IL-β-induced inflammatory OA model using in vitro cell experiments. PTE plays a role in the treatment of OA by inhibiting PI3K/AKT/NF-κB signaling pathway and reducing the expression of SASP.

Acknowledgements

Disclosure of conflict of interest

None.

Address correspondence to: Lunhao Bai, Department of Orthopedic Surgery, Shengjing Hospital Affiliated China Medical University, Sanhao Street 36#, Heping Area, Shenyang 110004, Liaoning Province, PR China. Tel: +86-13931403821; Fax: +86-13931403821; E-mail: bailh_sjhospital@126.com

References

[1] Barbour KE, Helmick CG, Boring M and Brady TJ. Vital signs: prevalence of doctor-diagnosed arthritis and arthritis-attributable activity limitation - United States, 2013-2015. MMWR Morb Mortal Wkly Rep 2017; 66: 246-253.

[2] Hunter DJ, March L and Chew M. Osteoarthritis in 2020 and beyond: a Lancet Commission. Lancet 2020; 396: 1711-1712.

[3] Wei Y and Bai L. Recent advances in the understanding of molecular mechanisms of cartilage degeneration, synovitis and subchondral bone changes in osteoarthritis. Connect Tissue Res 2016; 57: 245-261.

[4] Martel-Pelletier J, Barr AJ, Cicuttini FM, Conaghan PG, Cooper C, Goldring MB, Goldring SR, Jones G, Teichtahl AJ and Pelletier JP. Osteoarthritis. Nat Rev Dis Primers 2016; 2: 16072.

[5] Greene MA and Loeser RF. Aging-related inflammation in osteoarthritis. Osteoarthritis Cartilage 2015; 23: 1966-1971.

[6] Kelly PN. Targeting senescence to combat osteoarthritis. Science 2017; 356: 595-596.

[7] Franceschi C, Garagnani P, Parini P, Giuliani C and Santoro A. Inflammaging: a new immune-metabolic viewpoint for age-related diseases. Nat Rev Endocrinol 2018; 14: 576-590.

[8] Salotti J and Johnson PF. Regulation of senescence and the SASP by the transcription factor C/EBPβ. Exp Gerontol 2019; 128: 110752.

[9] Choi MC, Jo J, Park J, Kang HK and Park Y. NF-κB signaling pathways in osteoarthritic cartilage destruction. Cells 2019; 8: 734.

[10] Roman-Blas JA and Jimenez SA. NF-kappaB as a potential therapeutic target in osteoarthritis and rheumatoid arthritis. Osteoarthritis Cartilage 2006; 14: 839-848.

[11] Di Micco R, Krizhanovsky V, Baker D and d'Adda di Fagagna F. Cellular senescence in ageing: from mechanisms to therapeutic opportunities. Nat Rev Mol Cell Biol 2021; 22: 75-95.

[12] Birch J and Gil J. Senescence and the SASP: many therapeutic avenues. Genes Dev 2020; 34: 1565-1576.

[13] Herranz N and Gil J. Mechanisms and functions of cellular senescence. J Clin Invest 2018; 128: 1238-1246.

[14] Yang W, Sun C, He SQ, Chen JY, Wang Y and Zhuo Q. The efficacy and safety of disease-modifying osteoarthritis drugs for knee and hip osteoarthritis-a systematic review and network meta-analysis. J Gen Intern Med 2021; 36: 2085-2093.

[15] Kloppenburg M and Berenbaum F. Osteoarthritis year in review 2019: epidemiology and therapy. Osteoarthritis Cartilage 2020; 28: 242-248.

[16] Cameron M and Chrubasik S. Oral herbal therapies for treating osteoarthritis. Cochrane Database Syst Rev 2014; 2014: Cd002947.

[17] Zhang B, Tian L, Xie J, Chen G and Wang F. Targeting miRNAs by natural products: a new way for cancer therapy. Biomed Pharmacother 2020; 130: 110546.

[18] Sun K, Luo J, Jing X, Xiang W, Guo J, Yao X, Liang S, Guo F and Xu T. Hyperoside ameliorates the progression of osteoarthritis: An in vitro and in vivo study. Phytomedicine 2021; 80: 153387.

[19] Lu H, Fu C, Kong S, Wang X, Sun L, Lin Z, Luo P and Jin H. Maltol prevents the progression of osteoarthritis by targeting PI3K/Akt/NF-κB pathway: In vitro and in vivo studies. J Cell Mol Med 2021; 25: 499-509.

[20] Chen YL, Yan DY, Wu CY, Xuan JW, Jin CQ, Hu XL, Bao GD, Bian YJ, Hu ZC, Shen ZH and Ni WF. Maslinic acid prevents IL-1β-induced inflammatory response in osteoarthritis via PI3K/AKT/NF-κB pathways. J Cell Physiol 2021; 236: 1939-1949.

[21] Pérez-Lozano ML, Cesaro A, Mazor M, Esteve E, Berteina-Raboin S, Best TM, Lespessailles E and Toumi H. Emerging natural-product-based treatments for the management of osteoarthritis. Antioxidants (Basel) 2021; 10: 265.

[22] Li YR, Li S and Lin CC. Effect of resveratrol and pterostilbene on aging and longevity. Biofactors 2018; 44: 69-82.

[23] Blaker CL, Ashton DM, Doran N, Little CB and Clarke EC. Sex- and injury-based differences in knee biomechanics in mouse models of post-traumatic osteoarthritis. J Biomech 2021; 114: 110152.

[24] Nagira K, Ikuta Y, Shinohara M, Sanada Y, Omoto T, Kanaya H, Nakasa T, Ishikawa M, Adachi N, Miyaki S and Lotz M. Histological scoring system for subchondral bone changes in murine models of joint aging and osteoarthritis. Sci Rep 2020; 10: 10077.

[25] Arakawa K, Takahata K, Enomoto S, Oka Y, Ozone K, Nakagaki S, Murata K, Kanemura N and Kokubun T. The difference in joint instability affects the onset of cartilage degeneration or subchondral bone changes. Osteoarthritis Cartilage 2022; 30: 451-460.

[26] Ramos-Mucci L, Javaheri B, van 't Hof R, Bou-Gharios G, Pitsillides AA, Comerford E and Poulet B. Meniscal and ligament modifications in spontaneous and post-traumatic mouse models of osteoarthritis. Arthritis Res Ther 2020; 22: 171.

[27] Glasson SS, Blanchet TJ and Morris EA. The surgical destabilization of the medial meniscus (DMM) model of osteoarthritis in the 129/SvEv mouse. Osteoarthritis Cartilage 2007; 15: 1061-1069.

[28] Pritzker KP, Gay S, Jimenez SA, Ostergaard K, Pelletier JP, Revell PA, Salter D and van den Berg WB. Osteoarthritis cartilage histopathology: grading and staging. Osteoarthritis Cartilage 2006; 14: 13-29.

[29] Latourte A, Kloppenburg M and Richette P. Emerging pharmaceutical therapies for osteoarthritis. Nat Rev Rheumatol 2020; 16: 673-688.

[30] Jenei-Lanzl Z, Meurer A and Zaucke F. Interleukin-1β signaling in osteoarthritis - chondrocytes in focus. Cell Signal 2019; 53: 212-223.

[31] Dai SM, Shan ZZ, Nakamura H, Masuko-Hongo K, Kato T, Nishioka K and Yudoh K. Catabolic stress induces features of chondrocyte senescence through overexpression of caveolin 1: possible involvement of caveolin 1-induced down-regulation of articular chondrocytes in the pathogenesis of osteoarthritis. Arthritis Rheum 2006; 54: 818-831.

[32] Gao SG, Zeng C, Li LJ, Luo W, Zhang FJ, Tian J, Cheng C, Tu M, Xiong YL, Jiang W, Xu M and Lei GH. Correlation between senescence-associated beta-galactosidase expression in articular cartilage and disease severity of patients with knee osteoarthritis. Int J Rheum Dis 2016; 19: 226-232.

[33] Sikora E, Bielak-Zmijewska A and Mosieniak G. A common signature of cellular senescence; does it exist? Ageing Res Rev 2021; 71: 101458.

[34] Si HB, Yang TM, Li L, Tian M, Zhou L, Li DP, Huang Q, Kang PD, Yang J, Zhou ZK, Cheng JQ and Shen B. miR-140 attenuates the progression of early-stage osteoarthritis by retarding chondrocyte senescence. Mol Ther Nucleic Acids 2020; 19: 15-30.

[35] Sessions GA, Copp ME, Liu JY, Sinkler MA, D'Costa S and Diekman BO. Controlled induction and targeted elimination of p16 (INK4a)-expressing chondrocytes in cartilage explant culture. FASEB J 2019; 33: 12364-12373.

[36] Pignolo RJ, Samsonraj RM, Law SF, Wang H and Chandra A. Targeting cell senescence for the treatment of age-related bone loss. Curr Osteoporos Rep 2019; 17: 70-85.

[37] Roger L, Tomas F and Gire V. Mechanisms and regulation of cellular senescence. Int J Mol Sci 2021; 22: 13173.

[38] Meyer F, Dittmann A, Kornak U, Herbster M, Pap T, Lohmann CH and Bertrand J. Chondrocytes from osteoarthritic and chondrocalcinosis cartilage represent different phenotypes. Front Cell Dev Biol 2021; 9: 622287.

[39] Rim YA, Nam Y and Ju JH. The role of chondrocyte hypertrophy and senescence in osteoarthritis initiation and progression. Int J Mol Sci 2020; 21: 2358.

[40] Gorgoulis V, Adams PD, Alimonti A, Bennett DC, Bischof O, Bishop C, Campisi J, Collado M, Evangelou K, Ferbeyre G, Gil J, Hara E, Krizhanovsky V, Jurk D, Maier AB, Narita M, Niedernhofer L, Passos JF, Robbins PD, Schmitt CA, Sedivy J, Vougas K, von Zglinicki T, Zhou D, Serrano M and Demaria M. Cellular senescence: defining a path forward. Cell 2019; 179: 813-827.

[41] Zhao X, Huang P, Li G, Lv Z, Hu G and Xu Q. Activation of the leptin pathway by high expression of the long form of the leptin receptor (Ob-Rb) accelerates chondrocyte senescence in osteoarthritis. Bone Joint Res 2019; 8: 425-436.

[42] Xu L, Wu Z, He Y, Chen Z, Xu K, Yu W, Fang W, Ma C, Moqbel SAA, Ran J, Xiong Y and Wu L. MFN2 contributes to metabolic disorders and inflammation in the aging of rat chondrocytes and osteoarthritis. Osteoarthritis Cartilage 2020; 28: 1079-1091.

[43] Jiang Y. Osteoarthritis year in review 2021: biology. Osteoarthritis Cartilage 2022; 30: 207-215.

[44] López-Otín C, Blasco MA, Partridge L, Serrano M and Kroemer G. The hallmarks of aging. Cell 2013; 153: 1194-1217.

[45] Chakravarti D, LaBella KA and DePinho RA. Telomeres: history, health, and hallmarks of aging. Cell 2021; 184: 306-322.

[46] Franceschi C and Campisi J. Chronic inflammation (inflammaging) and its potential contribution to age-associated diseases. J Gerontol A Biol Sci Med Sci 2014; 69 Suppl 1: S4-9.

[47] Lagoumtzi SM and Chondrogianni N. Senolytics and senomorphics: natural and synthetic therapeutics in the treatment of aging and chronic diseases. Free Radic Biol Med 2021; 171: 169-190.

[48] Fafián-Labora JA and O'Loghlen A. Classical and nonclassical intercellular communication in senescence and ageing. Trends Cell Biol 2020; 30: 628-639.

[49] Jimi E, Fei H and Nakatomi C. NF-κB signaling regulates physiological and pathological chondrogenesis. Int J Mol Sci 2019; 20: 6275.

[50] Lepetsos P, Papavassiliou KA and Papavassiliou AG. Redox and NF-κB signaling in osteoarthritis. Free Radic Biol Med 2019; 132: 90-100.

[51] Sun K, Luo J, Guo J, Yao X, Jing X and Guo F. The PI3K/AKT/mTOR signaling pathway in osteoarthritis: a narrative review. Osteoarthritis Cartilage 2020; 28: 400-409.

[52] He L, Pan Y, Yu J, Wang B, Dai G and Ying X. Decursin alleviates the aggravation of osteoarthritis via inhibiting PI3K-Akt and NF-kB signal pathway. Int Immunopharmacol 2021; 97: 107657.

[53] Gómez-Zorita S, Milton-Laskíbar I, Aguirre L, Fernández-Quintela A, Xiao J and Portillo MP. Effects of pterostilbene on diabetes, liver steatosis and serum lipids. Curr Med Chem 2021; 28: 238-252.

[54] Xue EX, Lin JP, Zhang Y, Sheng SR, Liu HX, Zhou YL and Xu H. Pterostilbene inhibits inflammation and ROS production in chondrocytes by activating Nrf2 pathway. Oncotarget 2017; 8: 41988-42000.

[55] Mehta S, Young CC, Warren MR, Akhtar S, Shefelbine SJ, Crane JD and Bajpayee AG. Resveratrol and curcumin attenuate ex vivo sugar-induced cartilage glycation, stiffening, senescence, and degeneration. Cartilage 2021; 13 Suppl: 1214S-1228S.

[56] Vedadghavami A, Zhang C and Bajpayee AG. Overcoming negatively charged tissue barriers: Drug delivery using cationic peptides and proteins. Nano Today 2020; 34: 100898.

[57] Bajpayee AG and Grodzinsky AJ. Cartilage-targeting drug delivery: can electrostatic interactions help? Nat Rev Rheumatol 2017; 13: 183-193.

Pterostilbene ameliorates osteoarthritis through PI3K/AKT/NF-κB axis
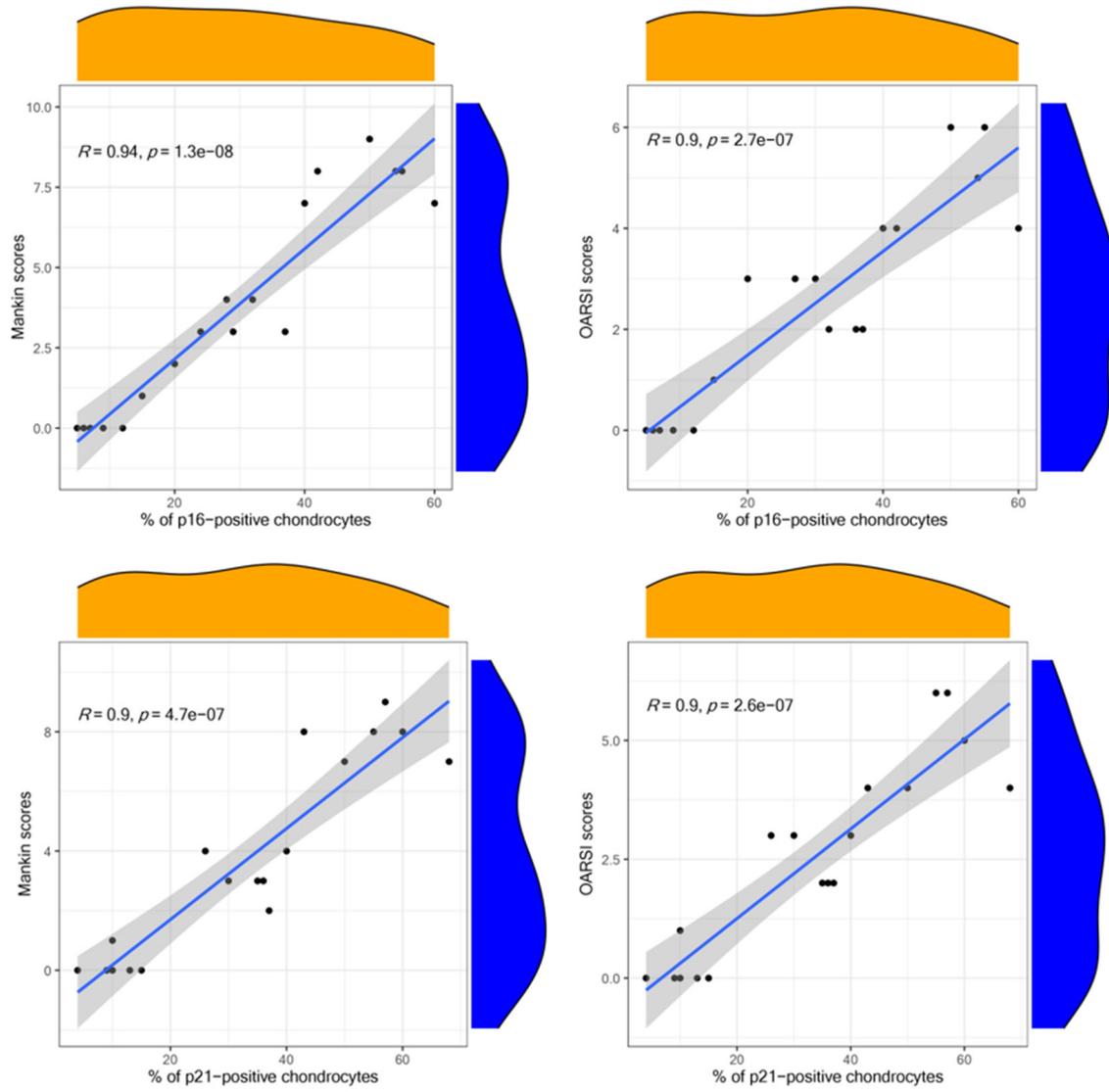
Figure S1. Correlation analysis of the ratio of positive cells for aging markers p16 and p21 with Mankin scores and OARSI scores showed that there was a significant positive correlation between them.

A

B

C
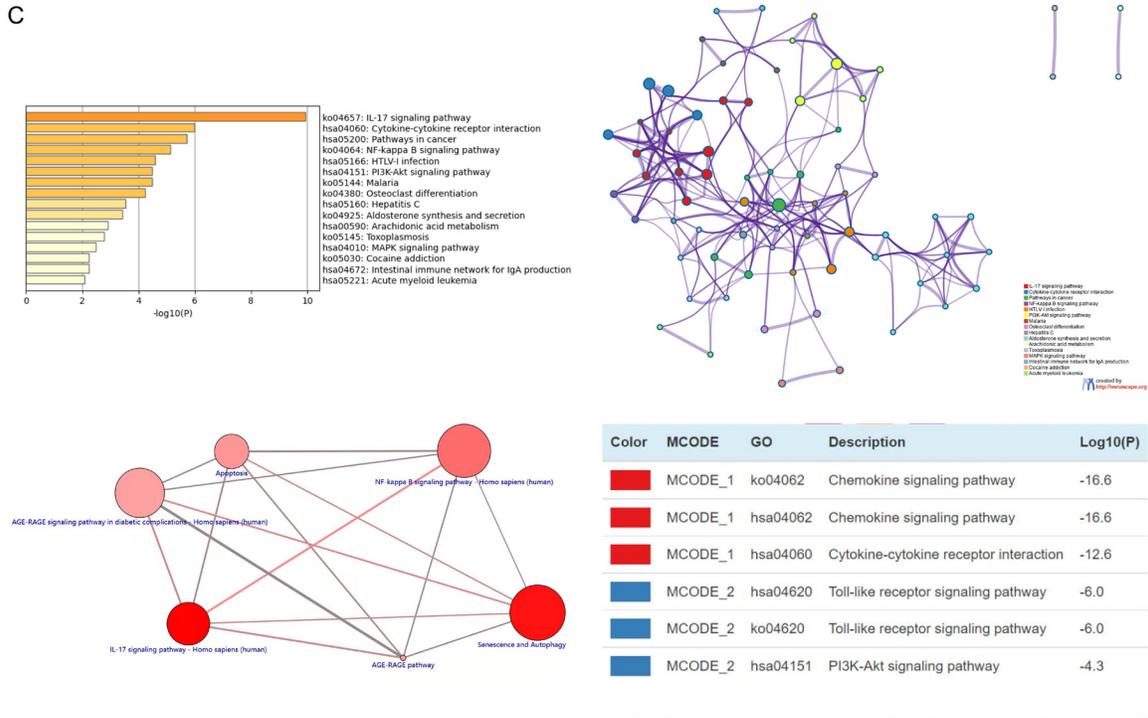
D
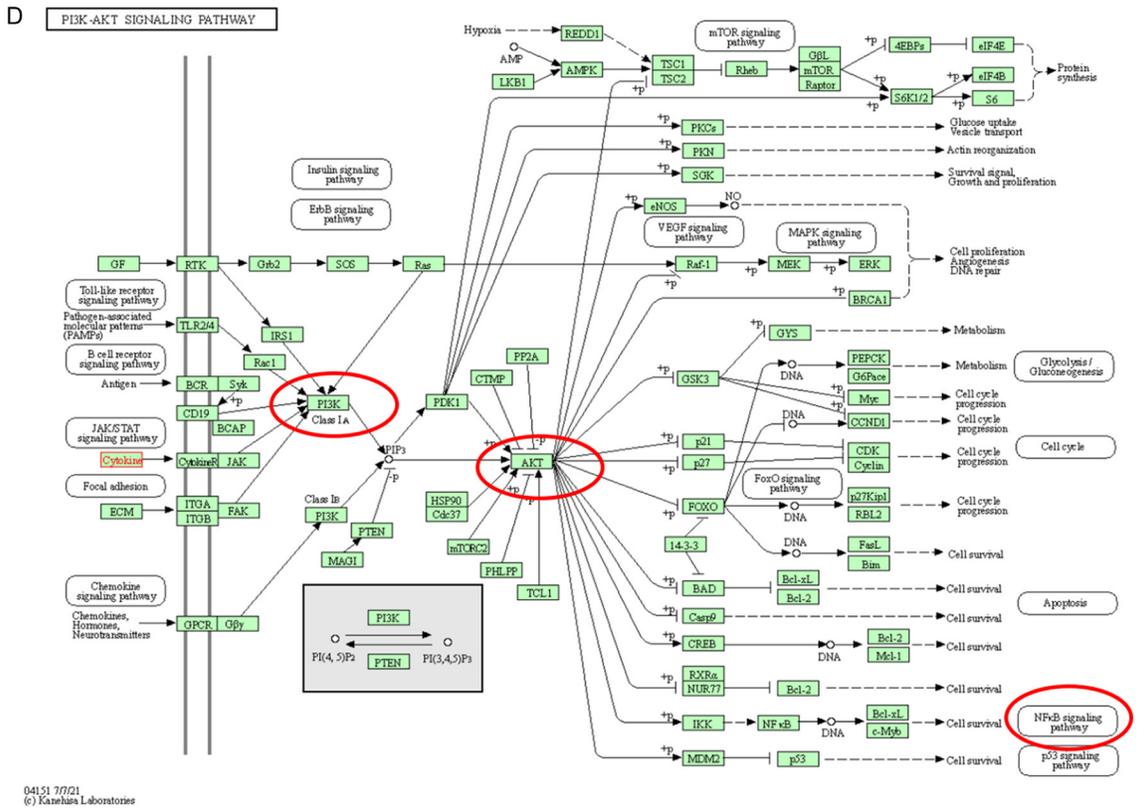
Figure S2. Bioinformatics analysis results showed the potential mechanism of PTE in the treatment of OA: regulating the PI3K/AKT/NF-κB signaling pathway axis inhibits the expression of SASP and plays an anti-inflammatory and anti-aging role in the treatment of OA.